Application of the Goda Pressure Formulae for Horizontal Wave Loads on Elevated Structures

Citation	Wiebe, D. M., Park, H., & Cox, D. T. (2014). Application of the Goda pressure formulae for horizontal wave loads on elevated structures. KSCE Journal of Civil Engineering, 18(6), 1573-1579. doi:10.1007/s12205-014-0175-1
DOI	10.1007/s12205-014-0175-1
Publisher	Springer
Version	Accepted Manuscript
Terms of Use	http://cdss.library.oregonstate.edu/sa-termsofuse

Application of the Goda Pressure Formulae for Horizontal Wave Loads on Elevated Structures

Dane M. Wiebe[*], Hyoungsu Park, and Daniel T. Cox*****

[*]Graduate Research Assistant, School of Civil and Construction Engineering, Oregon State University, Corvallis, Oregon, 97331, USA (E-mail: Wiebe@oregonstate.edu)

[**]Graduate Research Assistant, School of Civil and Construction Engineering, Oregon State University, Corvallis, Oregon, 97331, USA (Corresponding Author, E-mail: Hyoungsu.park@gmail.com)

[***]Professor, School of Civil and Construction Engineering, Oregon State University, Corvallis, Oregon, 97331, USA (E-mail: dan.cox@oregonstate.edu)

Abstract

Small-scale physical experiments were conducted to investigate the application of the Goda wave pressure formulae modified to predict the horizontal wave loads on elevated structures considering non-breaking, broken, and impulsive breaking waves. The air gap defined as the vertical distance from the still water level to the base of the structure played a key role in the reduction of wave impact forces. Physical model results using random waves confirmed that the modified application of the Goda wave pressure formulae provided a good estimate of the horizontal forces on elevated structures for both broken and impulsive breaking waves. As the air gap was increased, the resulting forces decreased, and the estimated values became increasingly conservative. When the ratio of the air gap to water depth, a/h', increased from -1.0 to 1.5, the reduction in force was approximately 75% when the wave height to breaking water depth ratio, H/h_b, was equal to unity.

Keywords: wave force; wave pressure; elevated structure; air gap; random waves; Goda; jetty

1. Introduction

Hurricanes can devastate coastal communities along the U.S. Gulf Coast. In 1900, a category 4 hurricane destroyed Galveston, Texas, killing 6000 people, and remains the single most deadly natural disaster in U.S. history. In 2005, Hurricane Katrina, a category 3 storms struck New Orleans, Louisiana, killing 1800 people, and caused an estimated $81 billion in damages, the most expensive natural disaster in U.S. history. On average, there are 6.2 hurricanes per year in the Atlantic Ocean, 1.7 of which make landfall along the U.S. coast (NOAA, 2012). These events often cause widespread damage as many structures near the coast are subjected to unexpected hydrodynamic loads from storm surge and waves which accompany hurricanes, and has been documented as the cause of wide spread failure of coastal highway bridges (Cuomo, *et al*., 2009; Robertson, *et al.*, 2007). Even structures sited well inland, such as residential dwellings, are susceptible if not elevated well above the maximum storm surge elevation. Building elevation has been found to be the critical parameter in determining a structures survival. For large wave climates, structures elevated above the storm surge are generally capable of survival and suffer relatively little damage, whereas structures located below it are generally completely destroyed. The relation between damage and elevation is so sensitive, that in some areas the difference between survival and destruction is only 0.5 m in elevation (Kennedy, *et al*., 2011).

Early research on elevated structures was performed by Bea *et al.* (1999), who studied the performance of platforms in the Gulf of Mexico which were subjected to several hurricane events. According to the design guidelines provided by the American Petroleum Institute, the decks of many of these platforms were lower than the storm wave crest heights, and should have been destroyed; however, some of these platforms survived while others failed. Based on the performance of these platforms, modifications to the design guidelines were suggested. The total force was a summation of buoyancy, horizontal slamming, horizontal hydrodynamic drag, vertical hydrodynamic uplift, and acceleration dependent inertia forces.

A more complicated mathematical model based on momentum was developed by Kaplan (1992), and Kaplan *et al.* (1995) to predict the time history of impact loadings on offshore platforms, and the wave impact force from large incident waves. The technique was similar to that used for modeling the ship slamming phenomena, based on Morrison’s equation, and accounted for hydrodynamic inertial forces, buoyancy forces, and drag forces. The theoretical horizontal force was combined total of the inertial momentum and drag.

More recently, Cuomo *et al.* (2007) conducted 1:25 scale model test of wave forces on exposed jetties. These tests focused on the physical loading processes, for both quasi-static and impulsive loading condition. Impulsive forces were found to reach values three times that of the corresponding quasi-static forces. Physical model results were compared to existing predictive formula (the momentum model) and found that the previous method had gaps and was inconsistent with the physics; therefore, new dimensionless predictive equations which are consistent with the physics were developed.

Inspired by the failure of coastal highway bridges during extreme storm events, Cuomo *et al.* (2009) performed large scale experiments, 1:10, on coastal highway bridges and determined the dynamics of wave loadings, the effects of openings in bridge decks, and derived predictive methods for both quasi-static and impulsive wave loads. The new predictive equations are intended for design, and account for the effects of impact duration.

Cuomo *et al.* (2010) also developed a predictive method for quasi-static and impact wave forces on vertical walls, which was derived from recent laboratory data collected for the Violent Overtopping by Waves at Seawalls (VOWS) project. The results were compared to previous studies and were found to provide a relatively good prediction. The new equations are similar in form to previous work by Cuomo et al. (2007) which are applicable to exposed jetties.

Wave forces on a 1:5 scale reinforced concrete causeway-type coastal bridge superstructure were investigated by Bradner *et al.* (2011) for a range of random and regular wave conditions, and water levels. The effect of wave height, wave periods, and water levels for both horizontal and vertical forces were investigated, and vertical force were found to be approximately four times greater than the horizontal force.

Formal design guidance for nearshore structures are published by both the American Society of Civil Engineers (ASCE) and the Federal Emergency Management Agency (FEMA). ASCE (2005) published minimum design standards for buildings and other structures, which include wave loads (Sections 5.4.2 to 5.4.5). In the ASCE standards, non-breaking and broken waves are treated as hydrostatic and hydrodynamic loads, with the hydrodynamic loads converted to an equivalent hydrostatic load based on a drag coefficient and the wave velocity. Breaking waves are treated as depth limited waves, and a combination of hydrostatic and dynamic pressures. FEMA (2011) published a design manual for residential coastal dwellings, which includes guidance on both wave forces, similar to those presented in the ASCE standards, and minimum structure elevations, which are set by local regulatory agencies and are often the minimum elevation required by the National Flood Insurance Program.

In summary, there is little consistent guidance for determining design wave loads on elevated structures in the nearshore, such as jetties, coastal highway bridges, or raised dwellings subject to wave loads. Most theories have been developed for either nearshore vertical walls or offshore elevated structures, and application of either of these methods to elevated structure in the nearshore may not be appropriate. Therefore, this paper investigates how well the existing and well-accepted formulae by Goda originally developed for caisson structures can be modified and applied for elevated structures. This paper is outlined as follows. Section 2 presents the modified application of the Goda wave pressure formulae. Section 3 compares the observed physical model results to theory. Section 4 concludes the paper with a concise summary of results.

2. The Goda Wave Pressure Formulae

Goda (1974; 2010) developed one of the most widely accepted methods for calculating wave forces on caissons, which assumes a trapezoidal pressure distribution (Fig. 1A). The formulae predict a maximum pressure at the still water level, p_1, which is directly proportional to the wave height, H, and is given by the following relation:

$$p_1 = \frac{1}{2}(1+cos\beta)(\alpha_1\lambda_1 + \alpha_2\lambda_2 cos^2\beta)\rho g H \qquad (1)$$

where β is the angle of wave incidence, ρ is the density of the water, g is the acceleration due to gravity, λ_1 and λ_2 are modification factors for structure geometry, and α_1 and α_2 are wave pressure coefficients. The pressure decreases linearly from p_1 at the SWL to p_2 at the depth in front of the breakwater, h. The pressure at the base of the armor layer, p_3, is determined by linearly interpolating between p_1 and p_2. The pressure at the structure crest, p_4, is determined by linearly interpolating between p_1 and the theoretical elevation above the still water where the pressure goes to zero, η^*.

The total horizontal force, F_h, acting on the vertical face of the caisson is calculated by integrating the pressure distribution over the corresponding area and is given by the following (for a structure where the freeboard exceeds η^*):

$$F_h = \frac{1}{2}(p_1)\eta^* + \frac{1}{2}(p_1 + p_3)h' \tag{2}$$

where h' is the water depth at the base of the armor layer.

The original formulae (Goda, 1974) did not address impulsive wave breaking. Therefore, Takahashi *et al.* (1994) modified the wave pressure coefficients, α_2, to account for impulsive conditions, which modified the pressure at the still water level, p_1 (Fig. 1A). While calculating pressure coefficients, α_2, we assumed that the berm width is zero, since our experiment performed on the plane slope without rubble mound.

In modifying Goda's formulae for elevated structures, two cases are considered. The first case shown in Fig. 1B is when the base of the structure is elevated above the bed but remains submerged below the SWL. The second case shown is Fig. 1C is when the base of the structure is elevated above the bed and is emergent above the SWL. Similar to the original case (Fig. 1A), the wave pressures p_1, p_2, p_3, and p_4 are assumed to remain constant. The pressure at the base of the elevated structure, p_5, is linearly interpolated using the following relation:

$$p_5 = \begin{cases} \left(1 - \dfrac{a}{\eta^*}\right) p_1 & \text{for} \quad a > 0 \\ \left(1 + \dfrac{a}{h'}\right)(p_1 - p_3) + p_3 & \phantom{\text{for}} \quad a \le 0 \end{cases} \tag{3}$$

where a is the air gap defined as the distance from the SWL to the base of the structure and the SWL such that $a < 0$ when submerged and $a > 0$ when emerged. These equations are intended for the case of zero overtopping, $h_c > \eta^*$. Fig. 1D shows a detail of the elevated structure for $a > 0$ with the parameters labeled. To calculate the total horizontal force, F_h, acting on the structure, the pressure distribution is integrated over the corresponding area. Note that the Goda wave pressure formulae are intended for sizing caisson breakwaters, and the input wave is supposed to be the highest wave height in the design sea state, H_{max}; however, for this work the individual wave forces from each wave are of interest, so H_{max} has been replaced with H. As well, note that the use of Eq. (3) with a/h' = -1 gives the original formula with the structure starting at the mudline (ie. no rubble mound base).

Fig. 2 shows the theoretical curves for both non-impulsive and impulsive non-dimensional horizontal wave force, $F_h/\rho g {h_b}^2$, as a function of non-dimensional wave height, H/h_b, for six non-dimensional air gaps, a/h', ranging from -1 to 1.5 using Eq. (3) and the assumption of no overtopping. Both the force and wave height are non-dimensionalized by the depth at breaking, and the air gap non-dimensionalized by the depth of water at the base of the structure. In both equations, there was a change in curvature near H/h_b = 0.8. This was attributed to the α_2 parameter which was taken as the minimum of two equations, and was the intersection of the two curves. As observed in Fig. 2, as the structure was elevated the trends of these lines remained well behaved, and the change in elevation simply provided a reduction in force. When the wave height to breaking depth ratio, H/h_b, was equal to unity, the theoretical reduction in force for each air gap case, a/h' = -0.5, 0.0, 0.5, 1.0, and 1.5 with respect to the resting on the bed cases, a/h' = -1.0, are 17, 35, 51, 66 and 77%, respectively. For each air gap case, the percent reduction in force decreased as wave heights increased (H/h_b ratio increased).

3. Experimental Description

In order to validate the modified Goda wave pressure formulae, a small-scale experiment was designed to measure the horizontal loads on an elevated structure. The experiment was conducted in a narrow flume which measured 487.5 cm long, 13.7 cm wide, and 32.2 cm deep, and had a piston type wave maker (Fig. 3). For these experiments, the bathymetry comprised of a horizontal section approximately 236.5 cm in length, followed by a 1:10 slope 190.0 cm in length. The load cell was suspended over the sloped portion of the bathymetry, approximately 332.5 cm from the maximum stroke position of the wave maker. Acoustic wave gages were placed over the horizontal portion of the flume, between the wave maker and sloped bathymetry, and over the sloped bathymetry, approximately 30.0 cm from the load cell ($5H_S$).

Random waves using the JONSWAP spectrum with γ = 3.3, H_S = 5.0 cm, and T_P = 1.5 s, were tested for 200 waves with a run time of 300 s. For this experiment ten different spectra with the same JONSWAP parameters were randomly generated, and the five spectra with the most similar significant wave heights (variation less than 0.7%) were chosen for further analysis, for a total of 1000 waves generated for each air gap. The start and end of each trail were truncated to eliminate transient effects. Therefore, approximately 193 of the 200 waves per trial for a total of 964 waves were used in the analysis at each of the six air gaps tested. The input wave conditions had a significant wave height, H_S = 5.79 cm, a peak period, T_P = 1.59 s, and a maximum wave height, H_{max} = 8.90 cm (Table 1).

For the experiment, the flume was held at a constant water depth, h = 17.0 cm. A load cell was placed in the middle of the breaking region, defined as the region were the majority of waves break, as to record non-breaking, broken, and breaking waves. The air-gap of the load cell was varied in 1.0 cm increments, from a = -2.0 cm (resting on the bed) to a = 3.0 cm above the still water level. Two acoustic wave gages were used to measure the free surface elevation at the flat section of the flume and approximately 5 wave heights in front of the load cell. Video records of each trial were used to classify the largest waves. The load cell was comprised of a flat aluminum plate which spanned the width of the flume and backed by four strain gages in each corner. In this way, the load cell gave a direct measure of the integrated pressure distribution although we did not account for the dynamic effects of the plate mass which was assumed negligible. The sampling frequency of load cell was 0.01 and mean strain gage value was calibrated at the start and end of the experiment.

Fig. 4 shows a scatter plot of the individual 964 waves plotted as h/gT^2 and H/gT^2 as measured by wave gage 1 for a/h' = 1.5. The results are similar for all a/h' ratios tested, and the value a/h' = 1.5 chosen as it was the highest air gap tested and had the least reflection. From this figure it is evident that the measured waves are at a transitional depth, and approaching the depth limited condition. The waves are scattered across multiple theories including Solitary, Cnoidal, and

Stokes II, III, and V order. The majority of the waves are categorized as Stokes II order, representative of realistic conditions. From this diagram it can be concluded that the waves were breaking due to the depth limited conditions rather than steepness limited conditions as would be expected in shallower water.

Fig. 5 shows a time series of non-dimensional free surface displacement, η/h_b, measured at wave gage 2 and non-dimensional forces, $F_h/\rho g {h_b}^2$, for a/h' = 1.0 for the first realization of waves. This figure shows the stochastic behavior of the horizontal wave forces in relation to the wave heights. The greatest forces are not necessarily associated with the largest waves, large waves may produce insignificant forces, and small waves are capable of generating significant forces. This variability is due to the location of breaking, and the compression of the entrained air pocket against the wall.

4. *Results and Discussions*

The following section presents observations, and a comparison between values from the physical experiment to the modified theory. Using video analysis, the highest one-tenth of waves (ranked by the corresponding force recorded on the load cell) were classified as non-breaking, broken, or breaking waves.

Non-breaking waves seldom ranked within the highest one-tenth, and generated relatively insignificant forces. When these waves contacted the base of the elevated structure, the crest of the waves was sheared off while the remainder of the wave continued to propagate by. As the air gap ratio, a/h', increased from -1.0 to 1.5, the overall number of non-breaking waves within the highest one-tenth increased from 2 to 14, and dramatically decreases the maximum horizontal force, $F_h/\rho g {h_b}^2$, 81% from 1.96 to 0.37. Broken waves generated the second largest forces, after breaking waves. Depending on the distance between the break point and the structure, the wave either broke in front of the structure and impacted as a violent splash, or broke some distance before the structure and arrived as a bore of water. As the air gap ratio, a/h', increased from -1.0 to 1.5, the overall number of breaking waves within the highest one-tenth increased from 51 to 74, and substantially decreased the maximum horizontal force, $F_h/\rho g {h_b}^2$ by 85% from 3.94 to 0.58.

As expected, breaking waves generated the largest forces of all wave types. When the wave broke just before the structure, the wave crest trapped a pocket of air against the wall even for these small-scale tests. The water compressed the air pocket as the wave collapsed until the air could burst upwards, which generated significantly more force than non-breaking and broken waves which did not trap air. As the air gap ratio, a/h', increased from -1.0 to 1.5, the overall number of breaking waves within the highest one-tenth decreased from 47 to 12, and dramatically decreased the maximum horizontal force, $F_h/\rho g {h_b}^2$, 75% from 6.12 to 1.50. Interestingly, the maximum number of breaking waves occurred for an air gap ratio of a/h' = -0.5, with 74 out of 100 waves. It is speculated that the slightly raised structure minimized wave reflection, provided a cleaner surf zone for incoming waves, and prevented premature breaking. Due to the compression of air against the structure, breaking waves are capable of increasing the force by a factor of three when compared to broken waves of similar height (H/h_b= 1.4, $F_{h_{brg}}/\rho g {h_b}^2$ = 6, $F_{h_{bkn}}/\rho g {h_b}^2$ = 2).

Fig. 6 shows the non-dimensional force, $F_h/\rho g {h_b}^2$, as a function of non-dimensional wave height, H/h_b, for the six air gap cases. Fig. 6F corresponds to the Goda formulae with no air gap, a/h' = -1.0, where the structure starts at the mudline, and Fig. 6E to A represent increasing air gap ratios from a/h' = -0.5 to 1.5. The experimental results show general agreement with the modified Goda formulae when compared at a/h' = -1.0. The modified non-impulsive formulae provide a reasonable estimate of non-breaking and broken wave forces, and the modified impulsive formulae provide a reasonable estimate of breaking wave forces (Fig. 6F). As the air gap is increased from resting on the bed to elevated well above the SWL, both of the modified theories continue to provide accurate estimates of the horizontal force (Fig. 6E to A).

The modified non-impulsive theory became increasingly conservative and overestimated the horizontal force for non-breaking and broken waves as the air gap ratio increased. The divergence was readily apparent at the largest air gaps (Fig. 6A and B). Due to the scarcity and scatter of breaking waves at the highest air gaps ratios, it is uncertain whether the modified impulsive theory also overestimates the breaking wave forces. For the higher air gaps ratios, the fundamental physical impact processes are changed. Therefore, instead stopping the full momentum of non-breaking and broken waves, it passes underneath the structure. For breaking waves, instead of air being trapped and compressed against the structure, the air is forced out underneath the structure.

5. Summary and Conclusions

The present paper investigated the application of the Goda wave pressure formulae to elevated structures, by carrying out small scale physical model tests. The waves were classified into three types, non-broken, broken, or breaking using video analysis and forces measured. Based on these observations from the small-scale flume with relative air gaps ranging from -1.0 < a/h' < 1.5, the air gap was found to play a key role in the reduction of horizontal wave forces. As expected, when the air gap increased, the resulting forces decreased, and the estimated value became increasingly conservative. As the a/h' ratio increased from -1.0 to 1.5, the reduction in force was approximately 75%, for H/h_b equal to unity. The physical model results confirmed that the modified application of the Goda wave pressure formulae provide a good estimate of the horizontal forces on elevated structures for impulsive breaking waves for all air gaps. For non-breaking and broken waves, the formulae were found to provide a good estimate for air gaps ranging from -1.0 < a/h' < 0, and provide a conservative estimate for a/h' > 0.

Overall, the results are encouraging but large scale model tests would be needed to confirm the applicability of Goda's formulae modified for elevated structures.

6. Acknowledgement

This material is based upon work partially supported by the National Science Foundation under Grant No. 13XXXXX. Any opinion, findings, and conclusions or recommendations expressed in this material are those of the authors and do not necessarily reflect the views of the National

Science Foundation. The authors thank two anonymous reviewers for their constructive comments. (NSF Grant No. is not currently unavailable due to the Shut Down. It will be updated before the final revision.)

7. References

ASCE, 2005. *Minimum design loads for buildings and other structures, ASCE/SEI 7-05,* Reston, VA: ASCE.

Bea, R. G., Xu, T., Stear, J. & Ramos, R., 1999. Wave forces on decks of offshore platforms. *Jounral of Waterway, Port, Coastal, and Ocean Engineering,* Vol. 125, No. 3, pp. 136-144.

Bradner, C., Schumacher, T. C. D. & Higgins, C., 2011. Experimental setup for a large-scale bridge superstructure model subjected to waves. *Journal of Waterway, Port, Coastal, and Ocean Engineering, ,* Vol. 137, No. 1, pp. 3-11.

Cuomo, G., Allsop, W., Bruce, T. & Pearson, J., 2010. Breaking wave loads at vertical seawalls and breakwaters. *Coastal Engineering,* Vol. 57, No. 4, pp. 424-439.

Cuomo, G., Shimosako, K. & Takahashi, S., 2009. Wave-in-deck loads on coastal bridges and the role of air. *Coastal Engineering,* Vol. 56, No. 8, pp. 793-809.

Cuomo, G., Tirindelli, M. & Allsop, W., 2007. Wave-in-deck loads on exposed jetties. *Coastal Engineering,* Vol. 54, No. 9, pp. 657-679.

FEMA, 2011. *Coastal Construction Manual: Principles and Practices of Planning, Siting, Designing, Constructing, and Maintaining Residential Buildings,* s.l.: FEMA.

Goda, Y., 1974. *New wave pressure formulae for composite breakwater.* Copenhagen, ASCE, pp. 1702-1720.

Goda, Y., 2010. *Random Seas and Design of Maritime Structures, 3rd Edition.* s.l.:World Scientific.

Kaplan, P., 1992. *Wave impact forces on offshore structures: Re-examination and new interpretations.* Houston, Texas, Offshore Technology Conference, pp. 79-86.

Kaplan, P., Murray, J. J. & Yu, W. C., 1995. Theorectical analysis of wave impact forces on platform deck structures. *Proceedings of the 14th International Conference on Offshore Mechanics and Arctic Engineering,* pp. 189-198.

Kennedy, A. et al., 2011. Building destruction from waves and surge on the Bolivar peninsula during Hurricane Ike. *Journal of waterway, port, coastal, and ocean engineering* , Vol. 13, No. 7, pp. 132-141.

NOAA, 2012. *Hurricane Research Division: Atlantic Oceanographic and Meteorological Laboratory*. Available at: http://www.aoml.noaa.gov/hrd/tcfaq/E11.html

Robertson, I. N., Riggs, H. R., Yim, S. C. S. & Young, Y. L., 2007. Lessons from Hurricane Katrina storm surge on bridge and buildings. *Journal of waterway, port, coastal, and ocean engineering*, Vol. 133, No. 6, pp. 463-483.

Takahashi, S., Tanimoto, K. & Shimosako, K., 1994. A proposal of impulsive pressure coefficient for the design of composite breakwaters. *Proclamation of the International Conference on Hydro-Technical Engineering for Port and Harbor Construction*, pp. 489-504.

Notation List

a	air gap
F_H	horizontal force
g	gravity
H	wave height
H_{max}	maximum wave height in the design sea state
H_S	significant wave height
h	depth of water in front of the breakwater
h'	depth of water above foundation
h_b	depth of water five wave heights seaward of the breakwater
h_c	freeboard
L	wavelength
N	number of waves
N_R	number of realizations
p	pressure
T_P	peak period
α	wave pressure coefficient
β	angle of wave incidence
γ	JONSWAP parameter
λ	modification factors for structure geometry
η^*	distance above SWL where pressure goes to zero
ρ	density

List of Figures

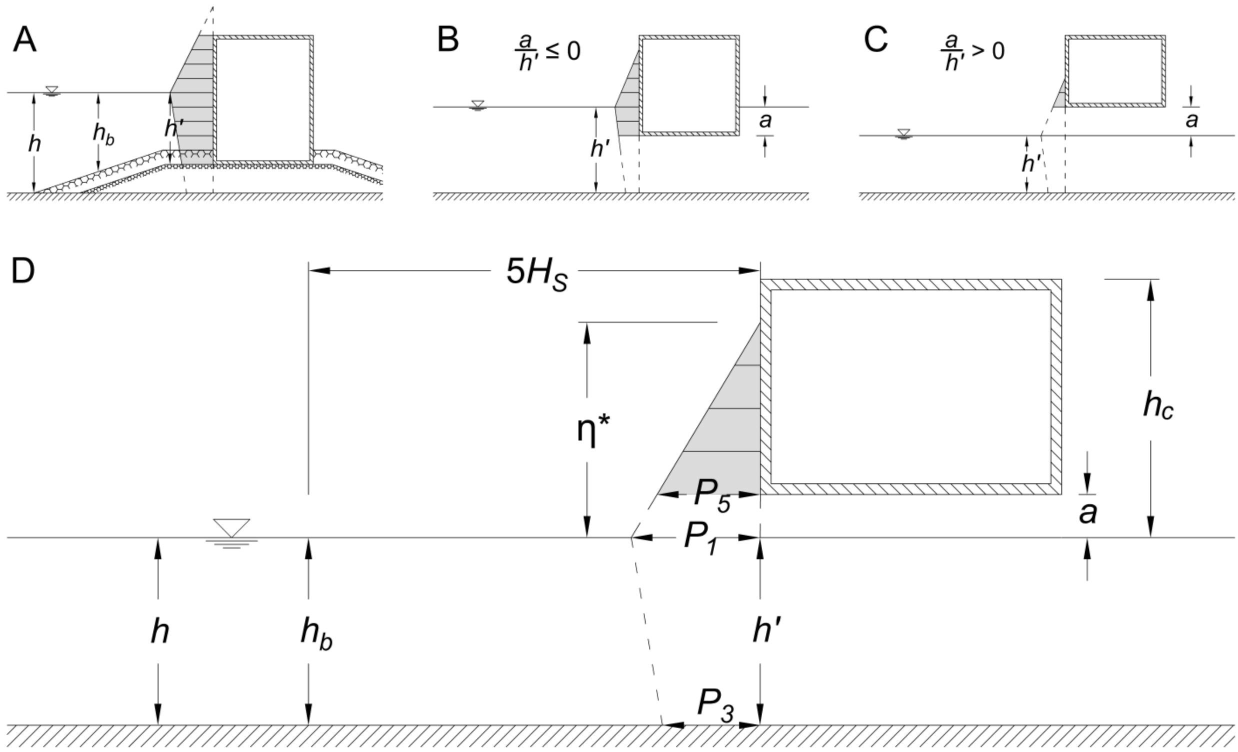

Fig. 1 Schematics of the Goda wave pressure distribution applied to: A) original application to a caisson type breakwater; B) modified for a structure submerged below sea level ($\mathrm{a}/h' \leq 0$); and C) modified for a structure elevated above sea level ($\mathrm{a}/h' > 0$). D) Detail of C for a structure elevated above sea level with labeled parameters.

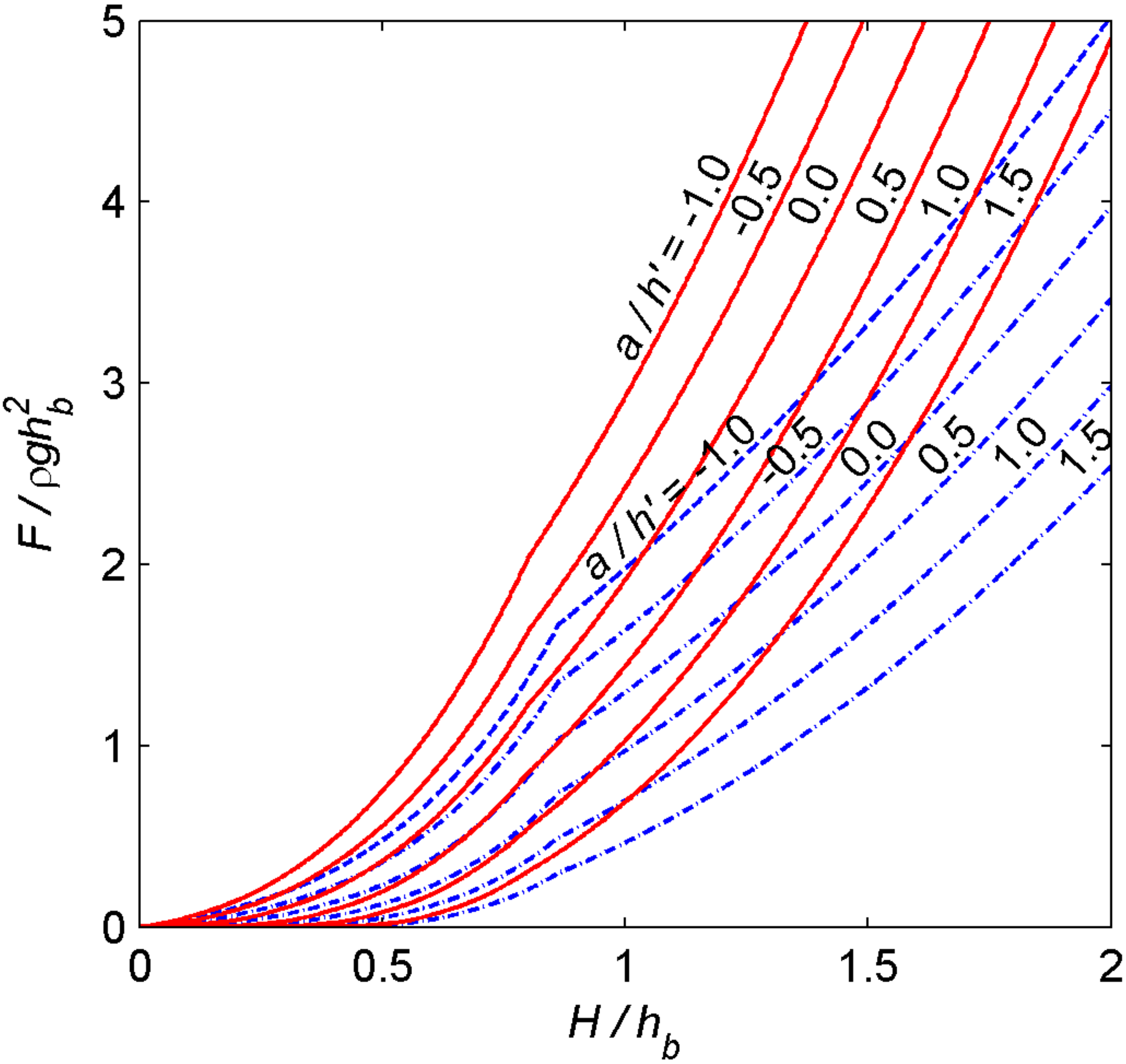

340

341 Fig. 2 Theoretical curves for non-impulsive (dash-dot) and impulsive (solid) horizontal wave forces

342 for the range of air gaps, -1 < a/h' < 1.5. The Goda formulae correspond to $\mathrm{a/h'}$ = -1.0.

343 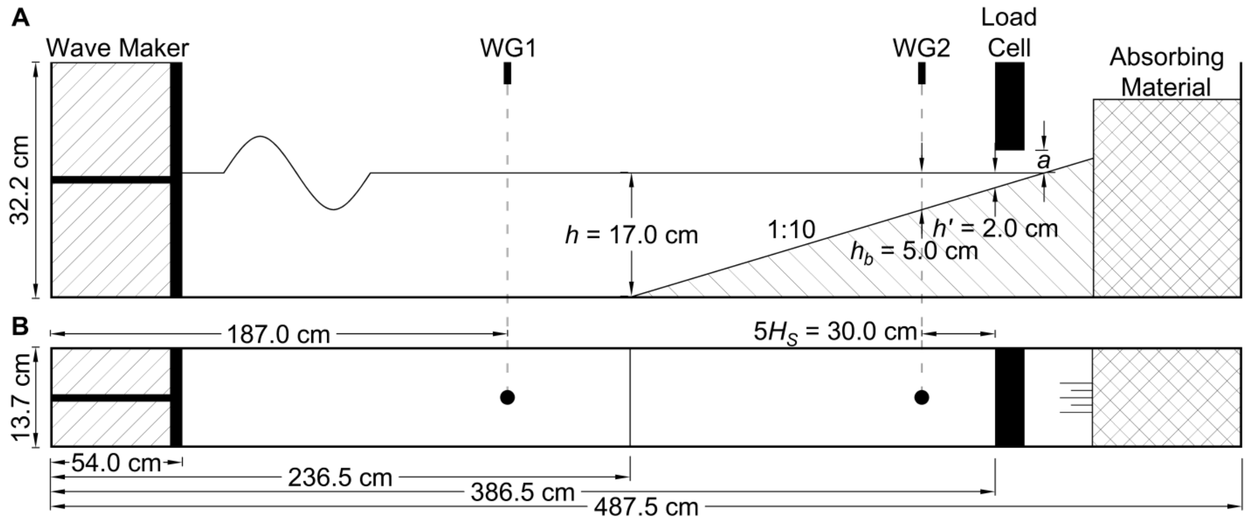

344 Fig. 3 Schematic of experimental configuration.

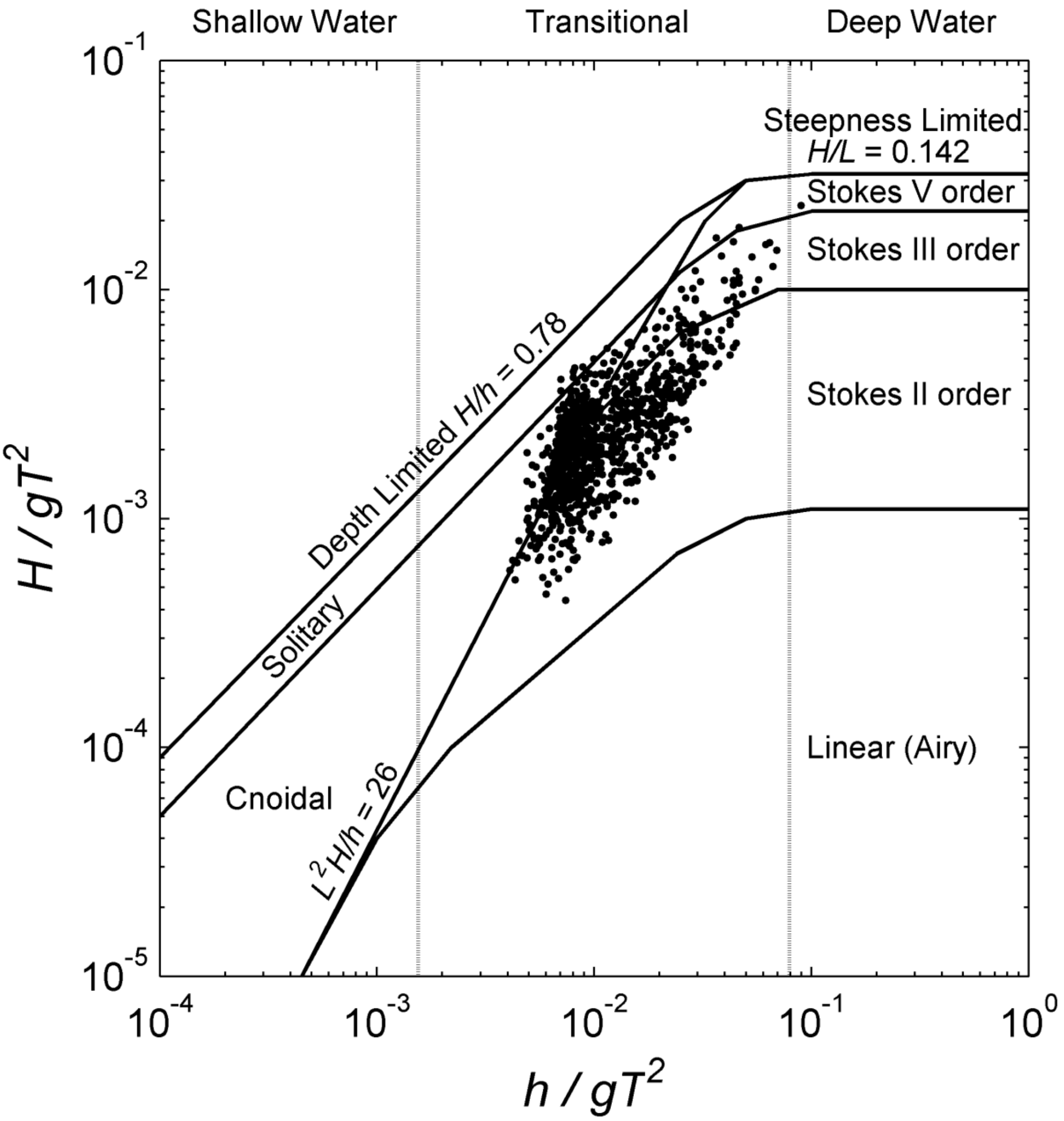

345

346 Fig. 4 Wave conditions for a/h′ = 1.5 (964 waves) measured at wave gage 1.

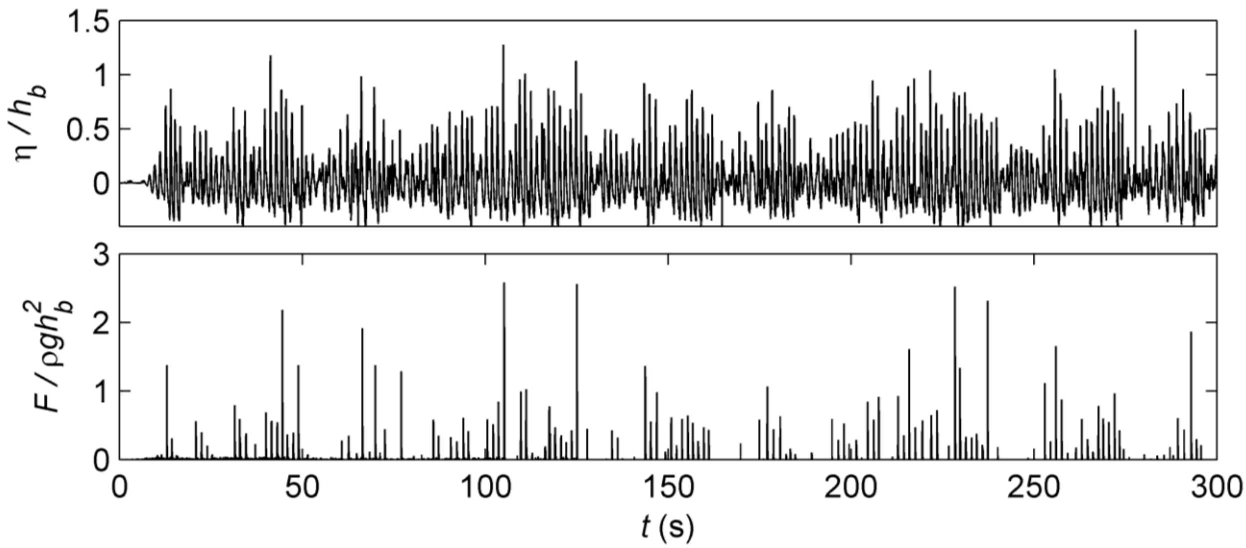

Fig. 5 Time series of free surface displacement (top) and force (bottom) for $a/h' = 1.0$, measured at wave gage 2.

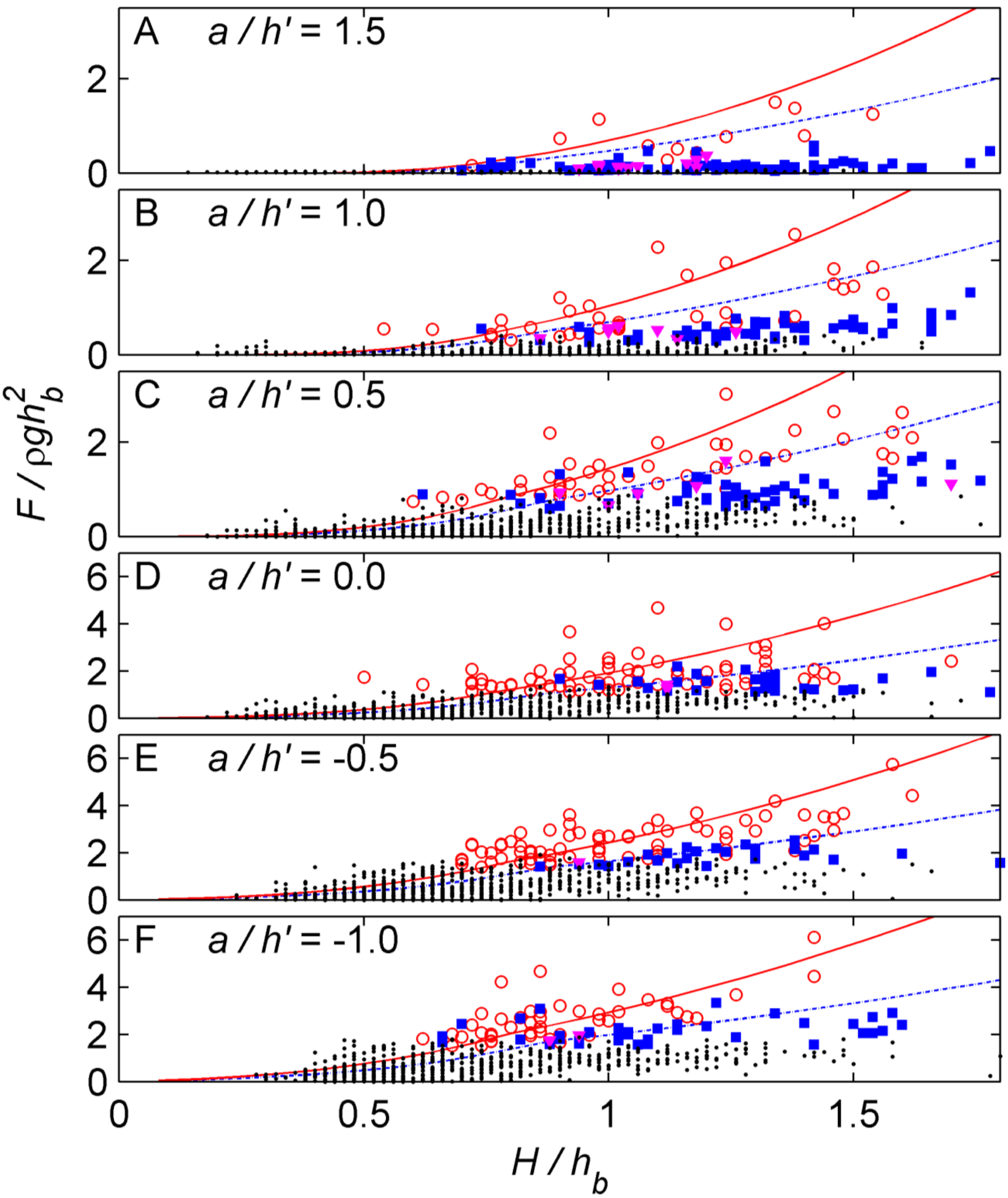

Fig. 6 Non-breaking (triangle), broken (square), breaking (circle) , and unclassified (dot) wave forces as a function of wave height for the six air gap cases compared to the modified theoretical impulsive (solid line) and non-impulsive (dash dot line) forces. Wave heights measured at wave gage 2.

List of Tables

Table 1. Summary of wave properties for the six test cases

Case	a/h'	N_R	N	H_s (cm)	T_p (s)	H/L	ξ
1	-1.0	5	964	5.99	1.57	0.0505	0.4449
2	-0.5	5	964	5.97	1.60	0.0495	0.4494
3	0.0	5	964	5.83	1.59	0.0493	0.4505
4	0.5	5	964	5.68	1.59	0.0485	0.4540
5	1.0	5	964	5.71	1.59	0.0486	0.4535
6	1.5	5	964	5.58	1.59	0.0482	0.4557
Avg.	-	-	964	5.79	1.59	0.0491	0.4513